Submitted, accepted and published by
Fuel Processing Technology 133 (2015) 210-219

Characterization of a Sol-gel Derived $CuO/CuAl_2O_4$ Oxygen Carrier for Chemical Looping Combustion (CLC) of Gaseous Fuels: Relevance of Gas-Solid and Oxygen Uncoupling Reactions

Daofeng Mei, [a] Alberto Abad, [*b] Haibo Zhao, [*a] Juan Adánez [b]

[a] State Key Laboratory of Coal Combustion, Huazhong University of Science and Technology, Wuhan 430074, People's Republic of China

[b] Department of Energy and Environment, Instituto de Carboquímica (ICB-CSIC), Miguel Luesma Castán 4, Zaragoza 50018, Spain

[*]Corresponding authors.
Tel.: +86 27 8754 4779x8208; Fax: +86 27 8754 5526.
E-mail address: klinsmannzhb@163.com (H. Zhao)
Tel.: +34 976 733977; fax: +34 976 733318.
E-mail address: abad@icb.csic.es (A. Abad).

Abstract

A new sol-gel $CuO/CuAl_2O_4$ material was characterized for chemical looping combustion (CLC) with gaseous fuels, including the analysis of the relevance of the oxygen uncoupling mechanism in oxygen transference was considered. This material possesses high reactivity and oxygen transport capacity, which combines the best features of the previously reported impregnated and spray-dried materials. A new test based on thermogravimetric analyzer (TGA) was designed and performed, from which the composition of this new material was determined. During the cycle tests in alternating N_2 and air, it was found that CuO decomposed fully into Cu_2O in N_2 and later completely regenerated to CuO in air, similarly to chemical looping with oxygen uncoupling (CLOU) for solid fuels. However, the decomposition of $CuAl_2O_4$ to $CuAlO_2$ was quite slow, and the followed regeneration of this compound cannot be accomplished. Subsequently, high numbers of cycles (>50 cycles) with gaseous fuels were conducted, which suggested adequate and stable rate for the combustion of the gaseous fuels with this oxygen carrier. The material undergone such cycles with gaseous fuels was then subjected to oxygen release and uptake cycles. It was observed that the $CuO/CuAl_2O_4$ was reconstructed after using in gaseous fuels combustion. This behavior resulted in the segregation of CuO from Al_2O_3 in the $CuAl_2O_4$, producing higher amount of free CuO and thus more available oxygen for CLOU with respect to the initial material. This is a new observation for this kind of material. Finally, the relative importance of gas-solid reactions in CLC against oxygen uncoupling in CLOU was examined when a fuel gas was presented in the reacting atmosphere, which, as one of the novelties of this paper, was never reported before.

Keywords: Chemical looping combustion (CLC); Chemical looping with oxygen uncoupling (CLOU); Sol-gel method; Cu-based oxygen carrier; CO_2 capture

1. Introduction

The greenhouse gas CO_2 has greatly increased its concentration over the past decades as a result of the dependence of energy produced from fossil fuels. It was reported that the global mean concentration of CO_2 had risen to 395 ppm in 2013 [1], which was increased more than 12% compared to the 1980s. Strategies are urgently needed to control the emission of CO_2, especially from the combustion of fossil fuel which provides 80% of the overall world consumption of energy. Analysis made by IPCC and IEA [2, 3] showed that the carbon capture and storage (CCS) could attribute 15-55% to the cumulative mitigation effort worldwide until 2100, to mitigate climate change to a reasonable cost. In this context, Chemical Looping Combustion (CLC) has been suggested among the best alternatives for the capture of CO_2 with low cost [4]. CLC concept based on the rationale of generating pure CO_2 was first proposed by Lewis and Gilliland [5]. This concept was recovered by Richter and Knoche in the 1980's as a highly efficient process for energy generation [6]. In CLC technology, combustion is split into separate reduction and oxidation: oxygen needed for the combustion of fuel is provided by one solid oxygen carrier, such as a metal oxide; and air is used to regenerate the oxygen carrier. Generally in CLC, the oxygen carrier circulates between interconnected fluidized-bed reactors to provide continuous oxygen source for the fuel combustion [7]. In one of the reactors, i.e. fuel reactor, the oxygen carrier is reduced and in another reactor, i.e. air reactor, the previously reduced oxygen carrier was continuously regenerated. As an alternative in CLC technology, Chemical Looping with Oxygen Uncoupling (CLOU), which was first proposed by Mattisson and coworkers [8], preserves the feasibilities of the CLC technology, but gaseous oxygen being generated in the fuel reactor. Thus, direct reaction between fuel and oxygen carrier particles is not required. In addition to the

properties of conventional CLC, the CLOU process gives higher conversion rates and efficiencies for the solid fuel combustion [9].

A schematic description of CLC technology, valid also for CLOU, is shown in Fig. 1 where the oxygen carrier, oxidized form MeO_x and reduced form MeO_{x-1}, circulates between the air and fuel reactors to provide the oxygen source for combustion. In the fuel reactor, the oxygen carrier MeO_x reacts with fuel (C_nH_{2m}) via reaction (1). Ideally, the outlet gas stream from the fuel reactor contains only CO_2 and H_2O (steam), where CO_2 can be easily separated by relatively inexpensive condensation of H_2O in the condenser. The reduced oxygen carrier MeO_{x-1} is subsequently transferred to the air reactor where it is regenerated for new cycles via reaction (2) by capturing O_2 from air. In CLC, the separation of CO_2 is inherently accomplished with low energy penalty and low cost. The concentrated CO_2 from CLC can be used for industrial purpose and the permanent underground storage [3]. In brief, the CLC technology provides a prospective technical strategy to address the global increasing of CO_2 emission.

Fuel reactor: $$C_nH_{2m} + (2n+m)\,MeO_x \longrightarrow (2n+m)\,MeO_{x-1} + n\,CO_2 + m\,H_2O \quad (1)$$

Air reactor: $$MeO_{x-1} + 1/2O_2(g) \longrightarrow MeO_x \quad (2)$$

The cornerstone of CLC and CLOU is the oxygen carrier used. Along with many other properties, the oxygen carrier must maintain the reactivity during long-term operation. In CLOU, special oxygen carriers are required to provide gaseous oxygen for the combustion of fuels [8, 10]. Based on the thermodynamic, the pairs CuO/Cu_2O, Mn_2O_3/Mn_3O_4, and Co_3O_4/CoO, can release and absorb oxygen at proper temperatures [8]. Among these oxides, CuO is highlighted for its high oxygen transport capacity, 10% with respect to 3% for Mn_2O_3 and 6.6% for Co_3O_4. Moreover, the reactions in fuel reactor and air reactor are exothermic when using the Cu-based materials, which

is beneficial to the heat balance over the global system [8, 11].

The earliest experimental investigation of CLOU was given by Mattisson et al. [12] by using a CuO supported on ZrO_2 material in a batch fluidized bed. In their experiments, petroleum coke burned quickly with the gaseous O_2 released from CuO/ZrO_2 particles. The average combustion rate of the petroleum coke varied between 0.5 and 5%/s depending on the temperature. This material was further demonstrated for its use in CLOU by combustions of six solid fuels (Mexican petroleum coke, South African coal, Indonesian coal, Colombian coal, German lignite and Swedish wood char) in the same batch fluidized bed reactor [13].

Researchers from ICB-CSIC developed Cu-based oxygen carriers with low attrition rate and high resistance to agglomeration both for CLC [14, 15] and for CLOU [16, 17]. For CLC, impregnated CuO/Al_2O_3 materials were extensively investigated in units ranging from 0.5 to 10 kW_{th}, even with sulphur containing gases [18-23]. These materials showed complete combustion of fuel gases due to the high reactivity with CH_4, H_2 and CO. In addition, agglomeration was avoided by maintaining the CuO content below 20 wt.% [14]. However, these impregnated CuO/Al_2O_3 materials have no or little CLOU properties [17].

For CLOU, more than 25 oxygen carriers prepared through various techniques was screened based on the following criterions: crushing strength, reactivity, resistance to attrition and agglomeration. After long-term tests, CuO supported on $MgAl_2O_4$ or ZrO_2 prepared by mechanical mixing followed by pelletizing by pressure were selected as suitable materials for CLOU. Subsequently, a similar material was demonstrated for the long-term use on CLOU in a 1.5 kW unit [11] with a bituminous coal as fuel. Later, combustion tests for several solid fuels, including anthracite, lignite and pine wood, were done [24-26]. Totally, 40 h for continuous combustion

under various conditions was accomplished. Complete combustion of the solid fuel was reached in all the cases and CO_2 capture rates higher than 95% were usually obtained.

Mei et al. recently developed a $CuO/CuAl_2O_4$ oxygen carrier by sol-gel [27, 28]. During their tests in batch fluidized bed reactor, the oxygen carrier composed of 60wt.% CuO and 40wt.% $CuAl_2O_4$ showed satisfactory properties for the combustion of different coals within 850-950 ^oC [28]. This oxygen carrier showed good properties to be used in the CLOU process. The sol-gel derived $CuO/CuAl_2O_4$ oxygen carrier maintained the porous structure after the tests with all the coals, which suggests that the sintering was avoided.

Additionally, the use of low-cost Cu based mineral as oxygen carrier would be very attractive. However, these materials agglomerated easily during fluidized bed operation, which makes difficult to find a proper mineral, excepting the recent work by Zhao et al. [29].

In the CLOU process with solid fuels, an excess of oxygen must be provided for the combustion in order to keep high carbon capture efficiency. This requirement was evidenced by the fact that small amount of O_2 was always mixed with the CO_2 stream outlet the fuel reactor. In this sense, Adánez-Rubio et al. identified the operational regions to give a mapping of the gas distribution under different solid inventories [30]. When the solid inventory was higher than 58 kg/MW_{th}, substantial O_2 was detected in the flue gas from fuel reactor meanwhile the full conversion to CO_2 was achieved. Decreasing the solid inventory to 32-58 kg/MW_{th}, the reduction of O_2 was attained; however, part of CO was not converted to CO_2. Moreover, CO in the exhaust gas increased together the depletion of oxygen, when oxygen carrier inventory in the fuel reactor was lower than 32 kg/MW_{th}. The results illustrate that there is a compromise between low oxygen carrier inventory and high purity of CO_2 in the CLOU combustion of coal. Thus, minor amount of either

O_2 or CO would be in the CO_2 stream. However, the actual solids inventory must also consider the combustion reactivity of solid fuel in order to get high CO_2 capture rates. Thus, preliminary calculations using kinetics for oxygen uncoupling reaction and coal combustion were performed. The results suggested that the solids inventory in the fuel reactor could be higher than 600 kg/MW_{th} to reach CO_2 capture higher than 95% for the lignite combustion [31]. Thus, an excess of oxygen would be expected in gas stream from fuel reactor, if both high CO_2 capture and complete fuel combustion was desired.

The oxygen uncoupling property of an oxygen carrier can be also exploited for gaseous fuel combustion [32-34]. It has been found that the CLC process can be highly improved when an oxygen carrier with CLOU properties and the appropriate operation windows were applied [34].

This work deals with the characterization of a new sol-gel derived $CuO/CuAl_2O_4$ oxygen carrier for its use in CLC of gaseous fuels, where the oxygen uncoupling involved in CLOU was studied as well. A thermogravimetric analyzer (TGA) was introduced to carry out the related experimental tests. The objectives of this work are: (*i*) a new material combining the best features of previously developed impregnated and spray-dried materials was characterized; (*ii*) a new way based on TGA test was detailed to determine the composition of the oxygen carrier; (*iii*) high numbers of cycles with gaseous fuels were performed for the new material; (*iv*) the oxygen uncoupling property of this new material was examined; (*v*) preliminary mechanistic of the segregation of CuO from Al_2O_3 in the $CuAl_2O_4$ was studied; .(*vi*) identification of the relative significance of CLC and CLOU effects was done when applying an oxygen-releasable material to gaseous fuel combustion.

2. Experimental

2.1. Oxygen carrier

The $CuO/CuAl_2O_4$ oxygen carrier material was prepared through the sol-gel technique which was usually used for preparing catalyst [35] and sometimes for the preparation of oxygen carrier particles being used for CLC technologies [28, 36-40]. This technique is highlighted for its advantages including: mixing precursors at the molecular level leads to homogeneous components, and controllable microstructure as a low-temperature synthesis. The precursors for Al and Cu elements in the product are aluminum isopropoxide [$Al(C_3H_7O)_3$, KESHI Co.] and copper nitrate [$Cu(NO_3)_2 \cdot 3H_2O$, Sinopharm Co.], respectively. Detailed description of the preparation process can be found in previous work [28] where a similar material containing 60 wt.% CuO and 40 wt.% $CuAl_2O_4$ was prepared. After crushing and sieving, the particles being sized to 125-180 μm were selected as oxygen carrier to be used in this work.

Composition of the sol-gel derived particles was summarized in Table 1. The phase composition of the oxygen carrier before and after use was identified using a Bruker AXS D8 Advance powder X-ray Diffraction (XRD) apparatus which is equipped with a graphite monochromator, using Ni-filtered "Cu Kα" radiation. The fresh oxygen carrier is composed of CuO and $CuAl_2O_4$ phases identified by XRD analysis. Elemental composition of Cu and Al was determined by inductively coupled plasma atomic emission spectroscopy (ICP-AES) with a Jobin Ybon 2000 apparatus, meanwhile the oxygen content was calculated for CuO and $CuAl_2O_4$ as major compounds. The total oxygen transport capacity was calculated for the full reduction of CuO and $CuAl_2O_4$ to Cu, being R_{OC}=11.6 wt.% from composition given by ICP-AES analysis.

The present oxygen carrier composed of CuO and $CuAl_2O_4$ has a special characteristic in terms of oxygen release and uptake. The critical condition of oxygen release depends on so-called O_2

equilibrium partial pressure. When the O_2 pressure in the atmosphere is lower than the equilibrium value, gaseous O_2 can be released via solid decompositions. In order to give a mapping of the present material, HSC Chemistry 6.1 [41] was used to calculate the O_2 equilibrium partial pressures of the CuO/Cu_2O system, while data from literature [42] was considered for the $CuAl_2O_4/CuAlO_2$ system. As shown in Fig. 2, both CuO and $CuAl_2O_4$ can give gaseous oxygen in proper conditions, albeit $CuAl_2O_4$ has lower O_2 equilibrium partial pressures. Additionally, previous works revealed that $CuAl_2O_4$ is reducible by syngas and methane [18, 43, 44] to Cu and Al_2O_3, but also reduced to $CuAlO_2$ in N_2 [17]. However, whereas reduced Cu can be regenerated to CuO and/or $CuAl_2O_4$, oxidation of $CuAlO_2$ to $CuAl_2O_4$ is impeded, likely due to oxygen diffusion limitations. To this end, CuO contained in the sol-gel derived $CuO/CuAl_2O_4$ oxygen carrier can provide one oxygen source for the CLC and CLOU process, but $CuAl_2O_4$ is expected to be active for oxygen transference in CLC, but not in CLOU in repeated redox cycles.

2.2. TGA tests

Experiments were carried out in a CI Electronics type thermogravimetric analyzer (TGA) with the $CuO/CuAl_2O_4$ material. A detailed description of the TGA can be found elsewhere [45]. The sample weight was around 50 mg for each test. The samples were first heated from 25 to 1000 ^oC at 20 ^oC/min in atmospheres either of 100 vol.% N_2 or 15 vol.% H_2 diluted by N_2 to analyze the oxygen uncoupling reaction or CuO-H_2 reaction, respectively. In this way, the available oxygen for CLOU and CLC was identified. Then, multiple redox cycles were conducted with reduction and oxidation agents at different temperatures in the 900-1000 ^oC interval. Reaction agents were 100 vol.% N_2, 15 vol.% H_2 or 15 vol.% CH_4 diluted by N_2 for reduction, and 100% air for

oxidation. In the case of the diluted CH_4, 20% steam was mixed to avoid the possible carbon deposition. In the above cycles, reaction periods are 15 min with N_2, 1 min with H_2 or CH_4 for reduction and 3 min with pure air for oxidation. Moreover, the evolution of the oxygen release and uptake properties relevant for CLOU mode of the $CuO/CuAl_2O_4$ material was analyzed. In this case, the particles being previously exposed to redox cycles with H_2 or CH_4 were tested in alternating air and N_2 atmosphere. Several tests were carried out varying the length of the former reduction periods using 5 vol.% H_2, which were followed by oxygen release and uptake cycles. In this way, the effect of the extension of gas-solid reactions -which are characteristics of the CLC process- on the oxygen evolution -distinctive of the CLOU process- was analyzed. In addition, experiments with lower H_2 concentration, 0.5-3 vol.%, were done at 950 ºC to evaluate the relevance of the oxygen uncoupling mechanism in the CuO reduction in presence of a fuel gas. For all the tests carried out at fixed temperatures, more than 10 cycles were operated to stabilize.

2.3. Data evaluation

To evaluate the $CuO/CuAl_2O_4$ oxygen carrier, the experimental data from TGA were processed to calculate the related parameters. The oxygen transport capacity, R_{OC}, was calculated for every relevant process with gaseous fuels, i.e. gas-solid reaction in CLC mode and oxygen uncoupling for the CLOU mode. Thus, $R_{OC,i}$ for CLC (i=CLC) and CLOU (i=CLOU) were calculated as $R_{OC,i}=(m_{ox}-m_{red,i})/m_{ox}$ where m_{ox} and $m_{red,i}$ denoted the mass of oxygen carrier in the oxidized and reduced form, respectively. $m_{red,CLC}$ and $m_{red,CLOU}$ depends on the application of the oxygen carrier, i.e. CLC or CLOU. For the $CuO/CuAl_2O_4$ material used in this work, $m_{red,CLC}$ corresponded to the complete reduction of $CuO/CuAl_2O_4$ to Cu and Al_2O_3, and $m_{red,CLOU}$ was related to the total

decomposition of CuO and $CuAl_2O_4$ to Cu_2O and $CuAlO_2$.

Solid conversion values were calculated for reduction/decomposition and oxidation process, respectively. Eq. (3.A) and Eq. (3.B) give the solid conversion $X_{\mathrm{red},i}$ during reduction and $X_{\mathrm{oxi},i}$ during oxidation with the subscript i discriminating CLC (i=CLC) and CLOU (i=CLOU). The m in Eq. (3.A) and Eq. (3.B) is the mass of oxygen carrier during the reactions.

$$X_{\mathrm{red},i} = \frac{m_{\mathrm{ox}} - m}{R_{\mathrm{OC},i} m_{\mathrm{ox}}} \tag{3.A}$$

$$X_{\mathrm{oxi},i} = 1 - \frac{m_{\mathrm{ox}} - m}{R_{\mathrm{OC},i} m_{\mathrm{ox}}} \tag{3.B}$$

Reaction rate of oxygen carrier was calculated through Eq. (4), where j=red and j=oxi refer to the reduction and oxidation, respectively.

$$(-r_{j,i}) = R_{\mathrm{OC,i}} \cdot \frac{dX_{j,\mathrm{i}}}{dt} \tag{4}$$

When using different concentrations of reduction agent, e.g. H_2, the reduction rate is considered to follow a n order with respect the H_2 concentration, C_{H_2}, as presented in Eq. (5).

$$-r_{red,CLC} = k_r C_{H_2}^n \tag{5}$$

where k_r is the apparent chemical reaction rate constant and n denotes the reaction order.

The mass variation during redox cycles was described by the normalized parameter ω, which represents the fraction of the changed mass during reactions with respect to the mass of the fully oxidized oxygen carrier, which was calculated as Eq. (6).

$$\omega = \frac{m}{m_{ox}} \tag{6}$$

3. Results

3.1. Temperature programmed reactions

In the temperature programmed reaction tests, the sol-gel derived oxygen carrier $CuO/CuAl_2O_4$ was characterized through temperature programmed reduction (TPR) with 15 vol.% H_2 and temperature programmed decomposition (TPD) in 100 vol.% N_2 to obtain the available oxygen contained in the material for CLC and CLOU, respectively. The reaction progresses of TPR and TPD are plotted in Fig. 3 with the temperature increasing from 25 to 1000 ^oC at 20 ^oC/min. More over, the $d\omega/dt$ as a function of temperature was considered to identify the stages of reactions, see the short-dash lines in Fig. 3. The reduction by 15 vol.% H_2 started at 300 ^oC and ended at 950 ^oC. It is composed of three stages, i.e. three peaks for the $d\omega/dt$ curve, which can be attributed to reduction of CuO to Cu, reduction of $CuAl_2O_4$ to $CuAlO_2$ and further reduction of $CuAlO_2$ to Cu and Al_2O_3. The mass-loss fraction involved in each process was 4.4 wt.% for the reduction of CuO to Cu, followed by an additional 6.6 wt.% for the reduction of $CuAl_2O_4$ to Cu and Al_2O_3. The final normalized mass-loss fraction was ω=0.89. Therefore, the oxygen transport capacity for the CLC process obtained through TGA experiments was $R_{OC,CLC}$=11%. This value was close to the 11.6 wt.% calculated by material composition determined by ICP-AES; see Table 1. Considering the mass-loss fraction values reacted during both CuO and $CuAl_2O_4$ reduction, it was calculated that the fraction of free CuO was 21.9 wt.%, whereas CuO in $CuAl_2O_4$ was 32.8 wt.%. This means that the total CuO in the particles was 54.7 wt.%, which is shared by 40 wt.% in free CuO and 60 wt.% in $CuAl_2O_4$, respectively. It is observed that the elemental composition determined by TGA has minor difference with respect to that from the ICP-AES analysis. The compounds for fresh material, which was determined based on the TPR test, were also shown in Table 1. CuO and $CuAl_2O_4$ were found as the main compounds, which was the same as that given by the XRD

analysis.

For the TPD reaction, considering the phase composition in Table 1, CuO and $CuAl_2O_4$ can be decomposed to Cu_2O and $CuAlO_2$, which resulted in two stages of reaction; see Fig. 3. The decomposition of CuO started at 850ºC and it can be considered to be finished at 940 ºC, i.e. when the slope in the mass-loss curve showed an abrupt decrease at $\omega \approx 0.98$. It is notable that the weight loss for this first stage of TPD curve is half of the reduction to Cu in the TPR curve, which is evident because the mass loss for CuO decomposition to Cu_2O is half of the fully reduction to Cu. Then, $CuAl_2O_4$ decomposes in 100 vol.% N_2 at a relatively low rate, which led to the incomplete decomposition of $CuAl_2O_4$, i.e. both $CuAl_2O_4$ and $CuAlO_2$ were found in the XRD analysis; see Table 1. In comparison to the TPD, different behavior of $CuAl_2O_4$ can be observed in TPR where $CuAl_2O_4$ was reduced to $CuAlO_2$, which led to the occurrence of the second peak of $d\omega/dt$, and then completely reduced to Cu and Al_2O_3 with reasonable rates, resulting in the last peak of $d\omega/dt$. From the TPD test, the final normalized mass-loss fraction was ω=0.967, although it could be lower for longer period. The theoretical oxygen transport capacity for the sol-gel derived $CuO/CuAl_2O_4$ oxygen carrier in CLOU mode was calculated to be $R_{OC,CLOU}$=5.5 wt.%.

3.2. Cycles with gaseous fuels

The reactivity and stability in the reaction with gaseous fuels are very important properties to evaluate an oxygen carrier. In this part, 50 and 10 cycles were performed with 15 vol.% H_2 and 15 vol.% CH_4, respectively, for the $CuO/CuAl_2O_4$ oxygen carrier. The solids conversion variation with time for each cycle was plotted in Fig. 4. With respect to the reductions, the oxygen carrier underwent a slow rate of conversion in the first cycle and then became stable during further cycles.

Independent of the gaseous fuels used, the oxygen carrier reached its maximum conversion within 35 seconds, indicating the same reactivity for both 15 vol.% H_2 and 15 vol.% CH_4 with $CuO/CuAl_2O_4$. Regarding the oxidation cycles, the stability of reaction was achieved since the first oxidation. In this sense, complete conversions of reductions and oxidations can be accomplished for the sol-gel derived $CuO/CuAl_2O_4$ oxygen carrier.

Fig. 5 shows the reaction rates for the 50 cycles with 15 vol.% H_2 and 100 vol.% air. It is observed that the reduction rate largely increased after the first cycle. Observation from the 2^{nd} to 25^{th} cycle indicates a slight increase of the reduction rate with the cycles, which might be attributable to a slight activation effect over the oxygen carriers. After that, a stable rate of oxygen transference $3.5 \cdot 10^{-3}$ $kgO_2/(s \cdot kgOC)$ was reached. This value is similar to the reduction rate by 15 vol.% H_2 for Cu-based materials prepared by impregnation on alumina, i.e. $3.1 \cdot 10^{-3}$ $kgO_2/(s \cdot kgOC)$ for Cu10Al material with 10 wt.% CuO [46] or $3.3 \cdot 10^{-3}$ $kgO_2/(s \cdot kgOC)$ for Cu14Al particles with 14 wt.% CuO [47, 48]. It is worth noting that the reacting time for impregnated materials is shorter than for sol-gel, but this is compensated by a higher CuO content, which must be also considered in the calculation of the oxygen transference rate; see Eq. (4). In a similar way, the oxygen transference rate was $3.5 \cdot 10^{-3}$ $kgO_2/(s \cdot kgOC)$ for the reductions by 15 vol.% CH_4, which is similar to the impregnated particles, namely $3.6 \cdot 10^{-3}$ $kgO_2/(s \cdot kgOC)$ for Cu10Al and $4.3 \cdot 10^{-3}$ for Cu14Al [46-48].

With respect of the oxidation, the oxygen carrier gained the stable reaction rates since the first oxidation. Only a slight increase of the oxidation rate was observed until 25^{th} cycle because of the activation effect. Similar to the reduction, high oxidation rates were obtained for the $CuO/CuAl_2O_4$ material, calculated to be $3.2 \cdot 10^{-3}$ $kgO_2/(s \cdot kgOC)$ for oxidation in air at 950 ºC. The

present sol-gel derived material exhibited similar rate of oxidation with respect to impregnated materials previously reported, namely $2.8 \cdot 10^{-3}$ $kgO_2/(s \cdot kgOC)$ for Cu10Al and $2.5 \cdot 10^{-3}$ $kgO_2/(s \cdot kgOC)$ for Cu14Al [46-48].

Based on the large numbers of tests with H_2 and CH_4, it was concluded that the sol-gel derived $CuO/CuAl_2O_4$ oxygen carrier can rapidly reach the stable reactivity with gaseous fuels during the cycle reactions. Therefore, for the sol-gel $CuO/CuAl_2O_4$, high and stable rates of reduction and oxidation were attained during the 50 cycles with H_2, CH_4 and air. This suggests that the present oxygen carrier possesses adequate rates for long-term use in CLC process. The sol-gel particles showed similar rates of oxygen transference than particles prepared by impregnation. It is noted that the Cu14Al material was successfully used in a 10 kW CLC unit for the combustion of CH_4 [19, 20]. In this sense, the oxygen carrier tested in the present work has adequate rates of both reduction and oxidation reactions to be used in CLC systems.

3.3. Cycles alternating N_2 and air

From TPD test in *Section 3.1*, it was concluded that the $CuO/CuAl_2O_4$ material can be proposed as an oxygen-releasable material because it decomposed to give gaseous oxygen in a N_2 atmosphere. Now, the oxygen uncoupling reaction was analyzed by isothermal tests in TGA. Fig. 6 shows 10 cycles of oxygen release and uptake, where the solids conversion evolution is presented as a function of time. As shown in Fig. 6.A, the decomposition of $CuO/CuAl_2O_4$ is consisted of a two-step process -a fast first reaction and a followed slow reaction- which corresponds to the oxygen releases from CuO and $CuAl_2O_4$, respectively, see also Fig. 3. Then the conversion does not reach the unity because of the slow decomposition of $CuAl_2O_4$ to $CuAlO_2$. In

addition, the oxidation process exhibits lower solid conversion than the decomposition, see Fig. 6.B, which can be related to the irreversible decomposition of $CuAl_2O_4$. Meanwhile it is notable that slow oxidation step was not noticed, see Fig. 6.B. Indeed, oxidation conversion was similar to the decomposition of CuO to Cu_2O in Fig. 6.A. Thus, re-oxidation of $CuAlO_2$ formed during reduction was not allowed, which was also observed by others in previous works [17, 44] with respect of Cu-based materials with Al_2O_3 as supports. When the number of redox cycles increased the decomposition of $CuAl_2O_4$ to $CuAlO_2$ was in progress. Eventually, final conversion for decomposition converged with oxidation conversion when all $CuAl_2O_4$ was decomposed into the inactive $CuAlO_2$.

Rates of $0.36 \cdot 10^{-3}$ $kgO_2/(s \cdot kgOC)$ for oxygen release and $1.3 \cdot 10^{-3}$ $kgO_2/(s \cdot kgOC)$ for oxidation were respectively attained at 950 ^oC. The rates of the present oxygen carrier, sol-gel derived $CuO/CuAl_2O_4$, are similar to $0.46 \cdot 10^{-3}$ $kgO_2/(s \cdot kgOC)$ for oxygen release and $1.8 \cdot 10^{-3}$ $kgO_2/(s \cdot kgOC)$ for oxidation of a spray-dried $CuO/MgAl_2O_4$ material at the same reaction conditions [31]. Considering the incomplete decomposition and oxidation of the $CuAl_2O_4$, the effective oxygen transport capacity was $R_{OC,CLOU}$=2.2 wt.%, which means that only the first 40 seconds in Fig. 6.B. could be significant for oxygen carrier regeneration. If this was considered, the $dX_{ox,i}/dt$ for the oxidation of Cu_2O to CuO was higher than the oxidation of Cu to CuO, see *Section 3.2.*, which indicated that the oxidation of Cu_2O is faster than the oxidation of Cu.

In CLOU, Cu_2O and $CuAlO_2$ were the final products after decomposition in N_2. However, the regeneration by air was possible only from Cu_2O to CuO, but not the $CuAl_2O_4$. Considering this, $CuAl_2O_4$ phase cannot be capable for oxygen generation, only the reduction of CuO to Cu_2O is available in oxygen uncoupling. Thus, the effective oxygen transport capacity for the sol-gel

derived $CuO/CuAl_2O_4$ oxygen carrier in CLOU was $R_{OC,CLOU}$=2.2 wt.% corresponding to the mass loss for CuO decomposition to Cu_2O.

The cycle tests in the above two sections, *Sections 3.2 and 3.3*, suggested both high reactivity and high oxygen transport capacity of the $CuO/CuAl_2O_4$ material. In this sense, the present sol-gel 22wt.%CuO+78wt.%$CuAl_2O_4$ material combined the best features of the previously reported impregnated and spray-dried oxygen carriers, Cu14Al [18-23] and Cu60MgAl [17].

3.4. Effect of reduction by fuel gas on decomposition in N_2

As it was stated above, the behavior in CLOU conditions is quite different than in CLC with H_2 or CH_4. On the one hand, the CLOU performance depends on the CuO and $CuAl_2O_4$ fraction because: (*i*) each reduction step in N_2 included a quick step and a followed slow step, respectively attributable to the decompositions of CuO to Cu_2O and $CuAl_2O_4$ to $CuAlO_2$; (*ii*) complete oxidation could not be attained, the non-oxidized fraction corresponding to the fraction of $CuAl_2O_4$ decomposed to $CuAlO_2$. On the other hand, in the reactions with gaseous fuels Cu and Al_2O_3 were the final products after the reductions with H_2, and later the Cu could be completely oxidized to CuO and/or $CuAl_2O_4$. Thus, the CLC performance does not depend on the CuO and $CuAl_2O_4$ fraction. However, once the Cu was formed, the fraction of CuO in the particles after oxidation could be different than the initial particles, because $CuAl_2O_4$ must be formed again by the dissolution of CuO on Al_2O_3. Then, the oxygen uncoupling properties of the oxygen carrier could vary with reduction cycles, as they shall depend on the fraction of copper as CuO.

To analyze the oxygen uncoupling performance of the materials with and without previous reductions by a fuel gas, several redox cycles were done alternating 100 vol.% N_2 and air. Fig. 7

presents in detail the mass variation obtained in 100 vol.% N_2 for fresh particles and for the particles previously undergone cycles with H_2. For fresh particles, the above described behavior was found, which was characterized by a two-step reduction -a fast reduction from CuO to Cu_2O and a followed slow decomposition of $CuAl_2O_4$-. It is worth to note that for the N_2/air cycles the final mass after the reduction period was decreasing with the cycle number, but the total mass loss was the same in each cycle. The total mass loss is related to the oxygen transport capacity; thus the oxygen transport capacity was constant throughout the redox cycles. If only the fast reaction rate was considered, corresponding to decomposition of CuO to Cu_2O, the oxygen transport capacity was calculated to be $R_{OC,CLOU}$=2.2 wt.%. For the tests at other temperatures, i.e. 900 and 1000 ^oC, the same effects on CLOU was observed.

In order to evaluate the influence of reduction with a fuel gas on the oxygen uncoupling performance, the oxygen carrier $CuO/CuAl_2O_4$ was exposed to successive cycles -50 cycles in 15 vol.% H_2, 5 cycles in 15 vol.% CH_4 and 5 cycles in 100 vol.% N_2. Fig. 8 shows the mass variations during these sequential reactions. The total duration of tests was 7 h, during which more than 5 h corresponds to the combustions of gaseous fuels. During the reduction by 15 vol.% H_2, higher extent of reduction was noticed after the 1st redox cycle because of slight activation effects; see also Fig. 5. Later, reactivity was constant up to 50th cycle. Then, the oxygen carrier exhibited the same mass variation with 15 vol.% CH_4+20 vol.% H_2O. The mass variation during redox cycles alternating H_2, or CH_4, and air was due to the total reduction of copper in the fresh sample to Cu^0, and re-oxidation to Cu^{2+}, corresponding to an oxygen transport capacity of $R_{OC,CLC}$=11 wt.%. Then, mass-loss fraction during decomposition in N_2 was 5.3 wt.% during the first cycle, i.e. approximately one half of the total mass-loss fraction with H_2 or CH_4. This means that near all

copper oxide was decomposed to Cu_2O. After that, oxygen carrier decomposition in 100 vol.% N_2 was found to be stable after the 3rd cycle, corresponding to $R_{OC,CLOU}$=4.9 wt.%. The above tests indicate that the sol-gel derived $CuO/CuAl_2O_4$ oxygen carrier possesses the CLOU ability after long-term of CLC process. Indeed, the oxygen transport capacity for CLOU was higher for particles which have been previously reduced by a fuel gas in comparison to fresh particles. This fact suggests that the $CuAl_2O_4$ formation from Cu oxidation was low.

More in detail, Fig. 7 presents the mass variations during the CLOU cycles of particles being previously exposed to cycles with H_2. For these particles, a quick decrease of mass fraction was observed which was followed by a rapid mass increase till around ω=1. This fact suggests that the reduction of any remaining $CuAl_2O_4$ was of low relevance, and only reduction of CuO to Cu_2O was observed. Moreover, the fast increase of mass fractions during oxidation is related to a rapid regeneration. It is notable that the re-oxidation resulted in the full regenerations, i.e. ω=1. Therefore, the mass variation in alternating N_2 and air for previously used with H_2 was quite different to that of fresh particles. This fact is related to the high segregation of CuO from Al_2O_3, as the fraction of $CuAl_2O_4$ formed during Cu or Cu_2O oxidation was low. It is valuable to mention that the decomposition and the regeneration of oxygen carrier used in the cycles with gaseous fuels had the same rates with the fresh particles. For the tests at other temperatures, i.e. 900 and 1000 ^oC, the same effects of CLC on CLOU were observed as well.

The following part tries to find the effect of the degree of reduction during CLC operation on the improvement of oxygen transport capacity for CLOU of the $CuO/CuAl_2O_4$ oxygen carrier. Controlling tests were carried out with low H_2 concentration, viz. 5 vol.% H_2, to reduce the oxygen carrier to different extents. The partial reduced particles were then oxidized and put into

alternating N_2 and air atmospheres to see the maximum oxygen release and uptake capacity. Fig. 9 plots the $X_{,red,CLOU}$ for oxygen release as a function of $X_{red,CLC}$ attained during the reduction cycles by gaseous fuels. At low levels of reduction by gas fuels, e.g. $X_{red,CLC}$<0.4, the $X_{red,CLOU}$ is around 0.5. However, when $X_{,red,CLC}$ was higher than 0.4 the $X_{red,CLOU}$ began to increase due to the higher available oxygen in the CuO form. It is necessary to emphasize that the $X_{red,CLC}$=0.4 determined by the composition in Table 1 corresponds to the beginning of the reduction of $CuAl_2O_4$, as seen from the vertical dash line in Fig. 9. In this sense, the reduction of $CuAl_2O_4$ to Cu and Al_2O_3 by a fuel gas occurred after the complete reduction of CuO to Cu, which gave extra CuO in the particles after oxidation. As a result, more CuO was produced via the reduction of $CuAl_2O_4$ to Cu with a gaseous fuel because the following oxidation of Cu forms CuO instead of $CuAl_2O_4$. The increasing amount of CuO in the oxygen carrier results in an increase of the active oxygen transport capacity for CLOU which also rises as higher degree of reduction with H_2 is reached. More indeed, the reduction of $CuAl_2O_4$ only occurred when the free CuO in the CuO/$CuAl_2O_4$ was totally reduced to Cu. Therefore, it can be speculated that in the fresh oxygen carrier the $CuAl_2O_4$ phase was covered by the CuO phase.

3.5. Relative significance of gas-solid reaction (in CLC) and oxygen uncoupling (in CLOU)

It is well known that the concentration of gaseous fuels affects the rate of reaction with oxygen carriers [46, 49, 50]. Thereby, H_2 concentrations in the reduction agent were varied from 0.5 vol.% to 15 vol.% to draw the influences on reduction process. Mass variations, ω, as a function of time were shown in Fig. 10 for different gas concentrations. According to previous results, different final weight losses were obtained for the decomposition in 100 vol.% N_2 than for reductions by H_2.

This fact was due to the different mechanisms involved in gas-solid reaction with a gaseous fuel and oxygen uncoupling in absence of a reducing agent, which are the main reactions involving the oxygen carrier in CLC and CLOU processes, respectively. Reduction in N_2 was mainly driven by CuO decomposition into Cu_2O, corresponding to a mass-loss fraction of 2.2 wt.% in fresh particles. However, regarding the reactions by gaseous fuel, no remarkable difference was found in the curves for the reduction from CuO to Cu_2O with respect to the reduction from Cu_2O to Cu, excepting the condition of 0.5 vol.% H_2. In the case of 0.5 vol.% H_2, a slight difference between the reduction of CuO to Cu_2O and the further reduction of Cu_2O to Cu was seen, that is, the slope of the reduction from CuO to Cu_2O was slightly higher than that of Cu_2O to Cu. Despite of this, complete reduction of the oxygen carrier by H_2 was reached during all the reduction tests by H_2.

Thus, regarding the reduction of CuO by H_2, the reaction rate decreased as the H_2 concentration decreased, which is not surprising. But more in detail, when the concentration of H_2 was lower than 1 vol.%, such as 0.5 vol.%, the reaction rate during CuO reduction to Cu_2O was equal to that obtained during the decomposition in pure N_2. This means the decrease of H_2 concentration in the interval lower than 1 vol.% cannot affect the rate of reaction from CuO to Cu_2O. This fact suggests a change on the mechanism for the reduction of CuO to Cu_2O when the H_2 concentration was changed to lower than 1 vol.%. To better identify those behaviors observed in Fig. 10, Fig. 11 shows a logarithmic plot for the reaction rate as a function of the H_2 concentration. As it was discussed previously, the rate of reaction with H_2 decreases as the fuel concentration decreases. It is valuable to note that a linear relation existed between $\ln(-r_{red,CLC})$ and $\ln C_{H_2}$ when the concentration of H_2 varied between values corresponding to 15 and 1 vol.%. Based on Eq. (5), the reaction order of H_2 during the reduction of $CuO/CuAl_2O_4$ to $Cu_2O/CuAl_2O_4$ was determined as

n=0.8.

However, when the H_2 concentration decreased below 1 vol.%, i.e. $\ln C_{H_2}$ <-2.3, a constant rate of reduction of 0.36×10^{-3} $kgO_2/(s\cdot kgOC)$ was observed, which is equal to the oxygen release rate calculated in *Section 3.3*. As a consequence, the oxygen uncoupling reaction is faster than the gas-solid reaction at low H_2 concentration, and therefore the oxygen transference rate was dominated by oxygen uncoupling mechanism. In this case, H_2 concentration exhibited little contribution to the rate of reaction.

As a comparison, the reduction rate for the complete reduction of $Cu_2O/CuAl_2O_4$ to Cu was calculated as well; see the red dots in Fig. 11. It is worth noting that it can not be distinguished the reduction of Cu_2O from the reduction of $CuAl_2O_4$. The reaction order obtained for the reduction of $Cu_2O/CuAl_2O_4$ to Cu is the same to the previous reduction, i.e. *n*=0.8, but higher than that obtained by García-Labiano et al. for an impregnated oxygen carrier [46], attributable to the different synthesis techniques.

As a conclusion, in the case of using a H_2 concentration higher than 1 vol.%, the effect of the gas-solid reaction is more relevant, and the reaction rate increases with H_2 concentration. In this sense, the H_2 concentration of 1 vol.% can be considered as a critical value. Higher concentration than 1 vol.% H_2 leads to faster oxygen transference rate via gas-solid reaction. In this case, combustion process would be dominated by common gas-solid reaction like those found for materials without oxygen uncoupling properties in CLC. On the contrary, oxygen uncoupling dominated the combustion of H_2, which means the oxygen transference rate is determined by the rate of oxygen release, whereas H_2 concentration contributes little to the reduction of CuO to Cu_2O. Nevertheless, the presence of H_2, even at low concentration values, allowed the full

reduction of the copper present in the particles to Cu^0 and then complete re-oxidition to Cu^{2+} was permitted, which is not the case for reduction for the oxygen uncoupling reaction in N_2.

The identification of CLC and CLOU is meaningful for the real application of oxygen-releasable materials to gaseous fuels combustion. It is known that the fuel concentration in the reactor can be decreased with the height of the reactor [47]. In this case, with this specific oxygen carrier CLC will dominate the fuel conversion process in the major part of the fuel reactor. However, CLOU can dominate in the upper part of the reactor, when the fuel gas was highly converted and its concentration was low. In this way, the complete conversion of the fuel can be facilitated by the CLOU mechanism. In this sense, for materials with lower rates of the gas-solid reaction the relative significance of CLOU over CLC could be more relevant that what was found for the $CuO/CuAl_2O_4$ material.

4. Conclusions

A new $CuO/CuAl_2O_4$ oxygen carrier prepared by sol-gel was studied in a thermogravimetric analyzer (TGA) for the chemical looping combustion of gaseous fuels, where the oxygen uncoupling process was also analyzed. This material combined the best features of the previously developed impregnated and spray-dried materials, Cu14Al and Cu60MgAl, which possessed both high reactivity and high oxygen transport capacity. For oxygen uncoupling, the free CuO in the $CuO/CuAl_2O_4$ can decompose and regenerate rapidly, whereas only slow decomposition of $CuAl_2O_4$ is feasible and the followed regeneration is incapable. During the gas-solid reaction, CuO and $CuAl_2O_4$ can be completely reduced to metallic Cu, where rather stable reactivity and adequate rates were obtained during more than 50 cycles. However, the followed re-oxidation of

Cu mainly towards CuO with minor $CuAl_2O_4$ formation. This can produce higher content of free CuO in the material. The new generated free CuO resulted in a higher effective oxygen transport capacity for the CLOU application. In the case of applying this kind of CLOU material to CLC for gaseous fuel combustion, the mode of reaction, i.e. CLC or CLOU, can be identified as a function of fuel gas concentration. In the case of H_2 combustion with $CuO/CuAl_2O_4$, a critical concentration of H_2, i.e. 1 vol.% H_2, was found, which determined either CLC or CLOU is the dominated mode for the gaseous fuel combustion. When the H_2 concentration was lower than 1 vol.%, the oxygen uncoupling effect was more relevant, and on the opposite the gas-solid reaction dominated, in the same way that with materials with no oxygen uncoupling property. It was the first time for the identification of CLC and CLOU effects for the combustion of gaseous fuels.

Acknowledgements

This work was supported by "National Natural Science Foundation of China (51390494)", and "National Basic Research and Development Program (2011CB707300)". Daofeng Mei is grateful for the support provided by the China Scholarship Council (CSC201306160054).

Nomenclature

C_{H_2}	H_2 concentration (mol/m^3)
k_r	Apparent chemical reaction rate constant, s^{-1}
m	Mass of oxygen carrier during the reaction processes, kg
m_{ox}	Mass of oxygen carrier in completely oxidized form, kg
$m_{red,i}$	Mass of oxygen carrier in completely reduced form, i=CLC or CLOU respectively for the application in CLC or CLOU, kg
n	Reaction order
$(-r_{j,i})$	Reaction rate of oxygen carrier, kgO_2/(s•kgOC)
$R_{OC,i}$	Oxygen transport capacity for CLC (i=CLC) or CLOU (i=CLOU), kgO_2/kgOC
t	Reaction time, s
$X_{j,i}$	Solid conversion during reduction (j=red) and oxidation (j=oxi) for CLC (i=CLC) and CLOU (i=CLOU)

Greek symbols

ω	Normalized mass variation

Acronyms

CLC	Chemical looping combustion
CLOU	Chemical looping with oxygen uncoupling
ICP-AES	Inductively coupled plasma atomic emission spectroscopy
OC	Oxygen carrier
TGA	Thermogravimetric analyzer
XRD	X-ray Diffraction

References

[1] NOAA-ESRL National Oceanic and Atmospheric Administration in the US, Average concentration of CO_2 in the atmosphere (Mauna Loa Observatory) for 2013 was posted June 14, 2014 (available at: http://www.esrl.noaa.gov/gmd/ccgg/trends/).

[2] IEA International Energy Agency, Energy technology perspectives, scenarios and strategies to 2050, OECD/IEA, Paris, 2010.

[3] IPCC, IPCC special report on carbon dioixde capture and storage, in: B. Metz, O. Davidson, H. de Coninck, M. Loos, L. Meyer (Eds.), Working Group III of the Intergovernmental Panel on Climate Change, Cambridge University Press, 2005.

[4] D.C. Thomas, H.R. Kerr, Capture and separation of carbon dioxide from combustion sources, in: D.C. Thomas, S.M. Benson (Eds.), Carbon dioxide capture for storage in deep geologic formations-results from the CO_2 capture project vol. 1, Elsevier, Oxford, 2005, pp. 583-586.

[5] W.K. Lewis, E.R. Gilliland, Production of pure carbon dioxide, Patent US 2665971, 1954.

[6] H.J. Richter, K.F.Knoche, Reversibility of combustion processes, in: R.A. Gaggioli (Ed), Efficiency and costing, ACS Symposium Series, Washington DC, 1983, pp. 71-85.

[7] A. Lyngfelt, B. Leckner, T. Mattisson, A fluidized-bed combustion process with inherent CO_2 separation: application of chemical-looping combustion, Chem. Eng. Sci. 56 (2001) 3101-3113.

[8] T. Mattisson, A. Lyngfelt, H. Leion, Chemical-looping with oxygen uncoupling for combustion of solid fuels, Int. J. Greenhouse Gas Control 3 (2009) 11-19.

[9] J. Adánez, P. Gayán, I. Adánez-Rubio, A. Cuadrat, T. Mendira, A. Abad, F. García-Labiano, L.F. de Diego, Use of Chemical-Looping processes for coal combustion with CO_2 capture, Energy Procedia 37 (2013) 540-549.

[10] J. Adánez, A. Abad, F. García-Labiano, P. Gayán, L.F. de Diego, Progress in chemical-looping combustion and reforming technologies, Prog. Energy Combust. Sci. 38 (2012) 215-282.

[11] A. Abad, I. Adánez-Rubio, P. Gayán, F. García-Labiano, L.F. de Diego, J. Adánez, Demonstration of chemical-looping with oxygen uncoupling (CLOU) process in a 1.5kW_{th} continuously operating unit using a Cu-based oxygen-carrier, Int. J. Greenhouse Gas Control 6 (2012) 189-200.

[12] T. Mattisson, H. Leion, A. Lyngfelt, Chemical-looping with oxygen uncoupling using CuO/ZrO_2 with petroleum coke, Fuel 88 (2009) 683-690.

[13] H. Leion, T. Mattisson, A. Lyngfelt, Using chemical-looping with oxygen uncoupling (CLOU) for combustion of six different solid fuels, Energy Procedia 1 (2009) 447-453.

[14] L.F. de Diego, P. Gayán, F. García-Labiano, J. Celaya, A. Abad, J. Adánez, Impregnated CuO/Al_2O_3 oxygen carriers for chemical-looping combustion: Avoiding fluidized bed agglomeration, Energy Fuels 19 (2005) 1850-1856.

[15] L.F. de Diego, F. García-Labiano, J. Adánez, P. Gayán, A. Abad, B.M. Corbella, J.M. Palacios, Development of Cu-based oxygen carriers for chemical-looping combustion, Fuel 83 (2004) 1749-1757.

[16] I. Adánez-Rubio, P. Gayán, F. García-Labiano, L.F. de Diego, J. Adánez, A. Abad, Development of CuO-based oxygen-carrier materials suitable for chemical-looping with oxygen uncoupling (CLOU) process, Energy Procedia 4 (2011) 417-424.

[17] P. Gayán, I. Adánez-Rubio, A. Abad, L.F. de Diego, F. García-Labiano, J. Adánez, Development of Cu-based oxygen carriers for chemical-looping with oxygen uncoupling (CLOU) process, Fuel 96 (2012) 226-238.

[18] C.R. Forero, P. Gayán, L.F. de Diego, A. Abad, F. García-Labiano, J. Adánez, Syngas combustion

in a 500 W_{th} chemical-looping combustion system using an impregnated Cu-based oxygen carrier, Fuel Process. Technol. 90 (2009) 1471-1479.

[19] J. Adánez, P. Gayán, J. Celaya, L.F. de Diego, F. García-Labiano, A. Abad, Chemical looping combustion in a 10 kW_{th} prototype using a CuO/Al_2O_3 oxygen carrier: Effect of operating conditions on methane combustion, Ind. Eng. Chem. Res. 45 (2006) 6075-6080.

[20] L.F. de Diego, F. García-Labiano, P. Gayán, J. Celaya, J.M. Palacios, J. Adánez, Operation of a 10 kW_{th} chemical-looping combustor during 200 h with a $CuO–Al_2O_3$ oxygen carrier, Fuel 86 (2007) 1036-1045.

[21] C.R. Forero, P. Gayán, F. García-Labiano, L.F. de Diego, A. Abad, J. Adánez, Effect of gas composition in chemical-looping combustion with copper-based oxygen carriers: Fate of sulphur, Int. J. Greenhouse Gas Control 4 (2010) 762-770.

[22] C.R. Forero, P. Gayán, F. García-Labiano, L.F. de Diego, A. Abad, J. Adánez, High temperature behaviour of a $CuO/\gamma Al_2O_3$ oxygen carrier for chemical-looping combustion, Int. J. Greenhouse Gas Control 5 (2011) 659-667.

[23] P. Gayán, C.R. Forero, A. Abad, L.F. de Diego, F. García-Labiano, J. Adánez, Effect of Support on the behavior of Cu-based oxygen carriers during long-term CLC operation at temperatures above 1073 K, Energy Fuels 25 (2011) 1316-1326.

[24] I. Adánez-Rubio, A. Abad, P. Gayán, L.F. de Diego, F. García-Labiano, J. Adánez, Performance of CLOU process in the combustion of different types of coal with CO_2 capture, Int. J. Greenhouse Gas Control 12 (2013) 430-440.

[25] I. Adánez-Rubio, A. Abad, P. Gayán, L.F. de Diego, F. García-Labiano, J. Adánez, Biomass combustion with CO_2 capture by chemical looping with oxygen uncoupling (CLOU), Fuel Process.

Technol. 124 (2014) 104-114.

[26] I. Adánez-Rubio, A. Abad, P. Gayán, F. García-Labiano, L.F. de Diego, J. Adánez, The fate of sulphur in the Cu-based chemical looping with oxygen uncoupling (CLOU) process, Applied Energy 113 (2014) 1855-1862.

[27] D. Mei, H. Zhao, Z. Ma, W. Yang, Y. Fang, C. Zheng, Oxygen release kinetics and mechanism study on Cu-, Co-, Mn-based oxygen carrier, J. Fuel Chem. Technol. 41 (2013) 235-242.

[28] D. Mei, H. Zhao, Z. Ma, C. Zheng, Using the sol-gel-derived $CuO/CuAl_2O_4$ oxygen carrier in chemical looping with oxygen uncoupling for three typical coals, Energy Fuels 27 (2013) 2723-2731.

[29] H. Zhao, K. Wang, Y. Fang, J. Ma, D. Mei, C. Zheng, Characterization of natural copper ore as oxygen carrier in chemical-looping with oxygen uncoupling of anthracite, Int. J. Greenhouse Gas Control 22 (2014) 154-164.

[30] I. Adánez-Rubio, A. Abad, P. Gayán, L.F. de Diego, F. García-Labiano, J. Adánez, Identification of operational regions in the chemical-looping with oxygen uncoupling (CLOU) process with a Cu-based oxygen carrier, Fuel 102 (2012) 634-645.

[31] I. Adánez-Rubio, P. Gayán, A. Abad, F. García-Labiano, L.F. de Diego, J. Adánez, Kinetic analysis of a Cu-based oxygen carrier: Relevance of temperature and oxygen partial pressure on reduction and oxidation reactions rates in chemical looping with oxygen uncoupling (CLOU), Chem. Eng. J. 256 (2014) 69-84.

[32] M. Källén, P. Hallberg, M. Rydén, T. Mattisson, A. Lyngfelt, Combined oxides of iron, manganese and silica as oxygen carriers for chemical-looping combustion, Fuel Process. Technol. 124 (2014) 87-96.

[33] M. Rydén, D. Jing, M. Källén, H. Leion, A. Lyngfelt, T. Mattisson, CuO-based oxygen-carrier

particles for chemical-looping with oxygen uncoupling-experiments in batch reactor and in continuous operation, Ind. Eng. Chem. Res. 53 (2014) 6255-6267.

[34] A. Abad, P. Gayán, L.F. de Diego, F. García-Labiano, J. Adánez, K. Mayer, S. Penthon, Modelling a CLC process improved by CLOU and validation in a 120 kW unit, in: Proc. 11th Int. Conf. on Fluidized Bed Technol., Beijing, China, 2014.

[35] C.J. Brinker, G.W. Scherer, Sol-gel science: the physics and chemistry of sol-gel processing, Gulf Professional Publishing, 1990.

[36] D. Mei, A. Abad, H. Zhao, J. Adánez, On a highly reactive Fe_2O_3/Al_2O_3 oxygen carrier for in-situ Gasification Chemical Looping Combustion (iG-CLC), Energy Fuels (2014), DOI: 10.1021/ef501981g.

[37] M. Ishida, H. Jin, T. Okamoto, A fundamental study of a new kind of medium material for chemical-looping combustion, Energy Fuels 10 (1996) 958-963.

[38] A.M. Kierzkowska, C.D. Bohn, S.A. Scott, J.P. Cleeton, J.S. Dennis, C.R. Müller, Development of iron oxide carriers for chemical looping combustion using sol−gel, Ind. Eng. Chem. Res. 49 (2010) 5383-5391.

[39] H. Zhao, L. Liu, B. Wang, D. Xu, L. Jiang, C. Zheng, Sol-gel-derived $NiO/NiAl_2O_4$ oxygen carriers for chemical-looping combustion by coal char, Energy Fuels 22 (2008) 898-905.

[40] H. Zhao, D. Mei, J. Ma, C. Zheng, Comparison of preparation methods for iron-alumina oxygen carrier and its reduction kinetics with hydrogen in chemical looping combustion, Asia-Pacific J. Chem. Eng. 9 (2014) 610-622.

[41] HSC Chemistry 6.1, Chemical reaction and equilibrium software with thermochemical database and simulation module, Oututec Research Oy, 2008.

[42] K.T. Jacob, C.B. Alcock, Thermodynamics of $CuAlO_2$ and $CuAl_2O_4$ and phase equilibria in the

system Cu_2O-CuO-Al_2O_3, J. Am. Ceram. Soc. 58 (1975) 192-195.

[43] S.Y. Chuang, J.S. Dennis, A.N. Hayhurst, S.A. Scott, Development and performance of Cu-based oxygen carriers for chemical-looping combustion, Combust. Flame 154 (2008) 109-121.

[44] M. Arjmand, A.M. Azad, H. Leion, T. Mattisson, A. Lyngfelt, Evaluation of $CuAl_2O_4$ as an oxygen carrier in chemical-looping combustion, Ind. Eng. Chem. Res. 51 (2012) 13924-13934.

[45] J. Adánez, L.F. de Diego, F. García-Labiano, P. Gayán, A. Abad, J.M. Palacios, Selection of oxygen carriers for chemical-looping combustion, Energy Fuels 18 (2004) 371-377.

[46] F. García-Labiano, L.F. de Diego, J. Adánez, A. Abad, P. Gayán, Reduction and oxidation kinetics of a copper-based oxygen carrier prepared by impregnation for chemical-looping combustion, Ind. Eng. Chem. Res. 43 (2004) 8168-8177.

[47] A. Abad, J. Adánez, F. García-Labiano, L.F. de Diego, P. Gayán, Modeling of the chemical-looping combustion of methane using a Cu-based oxygen-carrier, Combust. Flame 157 (2010) 602-615.

[48] A. Abad, P. Gayán, F. García-Labiano, L.F. de Diego, J. Adánez, Relevance of oxygen carrier characteristics on CLC design for gaseous fuels, in: Proc. 3rd Int. Conf. on Chemical Looping, Göteborg, Sweden, 2014.

[49] A. Abad, F, García-Labiano, L.F. de Diego, P. Gayán, J. Adánez, Reduction kinetics of Cu-, Ni-, and Fe-based oxygen carriers using syngas ($CO+H_2$) for chemical-looping combustion, Energy Fuels 21 (2007) 1843-1853.

[50] L.F. de Diego, A. Abad, A. Cabello, P. Gayán, F. García-Labiano, J. Adánez, Reduction and oxidation kinetics of a $CaMn_{0.9}Mg_{0.1}O_{3-\delta}$ oxygen carrier for chemical-looping combustion, Ind. Eng. Chem. Res. 53 (2014) 87-103.

Figure Captions

Fig. 1. Schematic layout of generic CLC process.

Fig. 2. Equilibrium O_2 concentration of Cu_2O/CuO and $CuAlO_2/CuAl_2O_4$ systems as a function of temperature.

Fig. 3. Mass variations, ω, and $d\omega/dt$ (short-dash lines) of the $CuO/CuAl_2O_4$ material during the TPR with 15%H_2 and the TPD with 100%N_2, temperature was increased from 25 to 1000 ^oC at 20 ^oC/min.

Fig. 4. Solids conversions as a function of reaction time for (A) 50 reductions with 15 vol.% H_2, (B) 50 oxidations with 100 vol.% air after reduction with H_2, (C) 10 reductions with 15 vol.% CH_4+20%H_2O, (D) 10 oxidations with 100 vol.% air after reduction with CH_4; temperature was fixed at 950 ^oC.

Fig. 5. Reaction rates of reduction and oxidation change as a function of cycle numbers during the redox by 15 vol.% H_2 and 100 vol. % air at 950 ^oC.

Fig. 6. Oxygen carrier conversions as a function of time during 10 cycles with (A) 100 vol.% N_2 and (B) 100 vol.% air; tests were conducted at 950 ^oC; Calculated using R_{OC} = 5.5 wt.%.

Fig. 7. Mass variations in CLOU process in cycles alternating N_2 and air for fresh $CuO/CuAl_2O_4$ (black line) and for particles after redox cycles with 15 vol.% H_2 (blue line). The operation temperature is 950 ^oC.

Fig. 8. Mass variations as a function of the reaction time for $CuO/CuAl_2O_4$ during 50 redox cycles with 15 vol.% H_2, followed by 5 cycles with 15 vol.% CH_4+20%H_2O and then 5 cycles with 100 vol.% N_2 at 950 ^oC; oxidation periods were conducted with 100 vol.% air.

Fig. 9. Solid conversions in 100 vol.% N_2, $X_{red,CLOU}$, as a function of the reduction degree $X_{red,CLC}$

with gaseous fuels attained in previous redox cycles; Temperature: 950 ^{o}C; $R_{OC,CLOU}$ = 5.5 wt.%.

Fig. 10. Effects of H_2 concentration on the reduction of the $CuO/CuAl_2O_4$ oxygen carrier; Temperature: 950 ^{o}C.

Fig. 11. Reduction rates of $CuO/CuAl_2O_4$ as a function of the H_2 concentration.

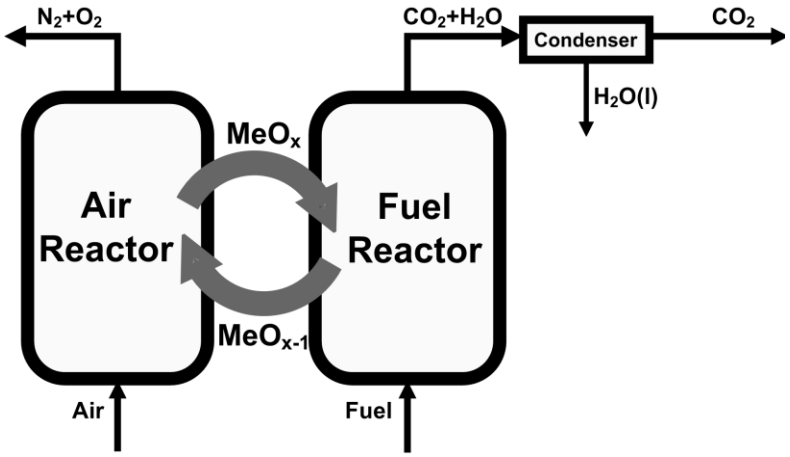

Fig. 1. Schematic layout of generic CLC process.

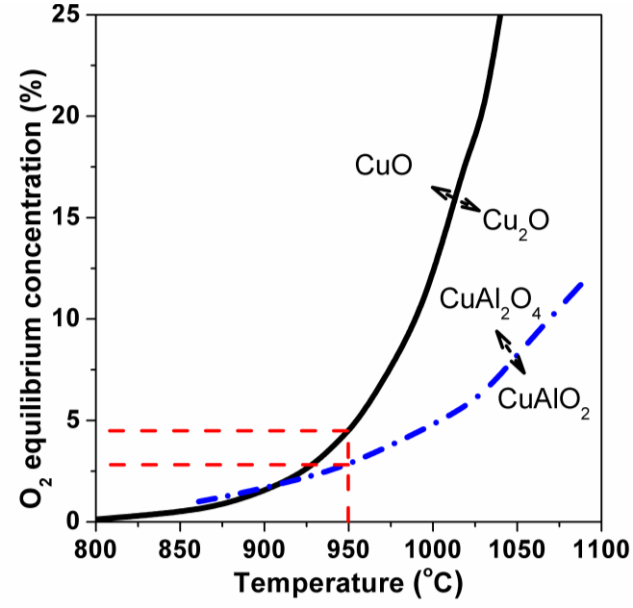

Fig. 2. Equilibrium O_2 concentration of Cu_2O/CuO and $CuAlO_2/CuAl_2O_4$ systems as a function of temperature.

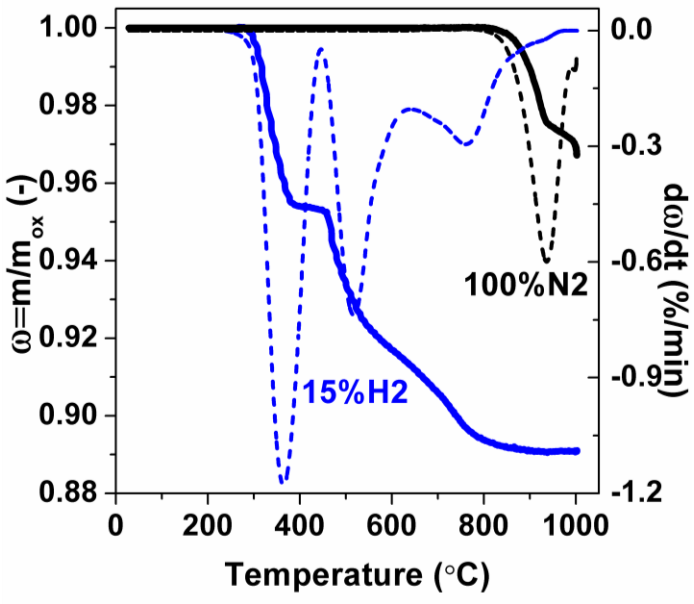

Fig. 3. Mass variations, ω, and $d\omega/dt$ (short-dash lines) of the $CuO/CuAl_2O_4$ material during the TPR with 15%H_2 and the TPD with 100%N_2, temperature was increased from 25 to 1000 ^oC at 20 ^oC/min.

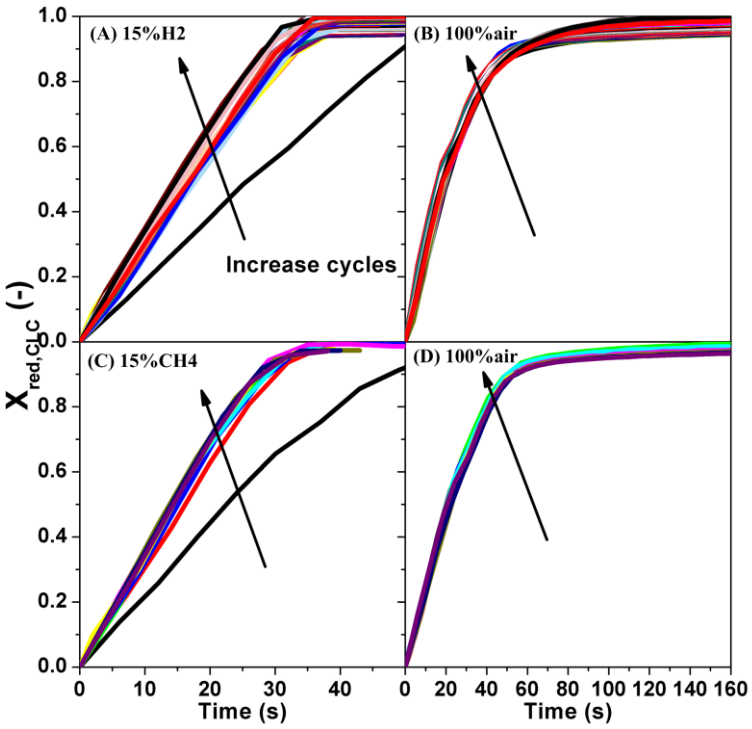

Fig. 4. Solids conversions as a function of reaction time for (A) 50 reductions with 15 vol.% H_2, (B) 50 oxidations with 100 vol.% air after reduction with H_2, (C) 10 reductions with 15 vol.% CH_4+20%H_2O, (D) 10 oxidations with 100 vol.% air after reduction with CH_4; temperature was fixed at 950 ^oC.

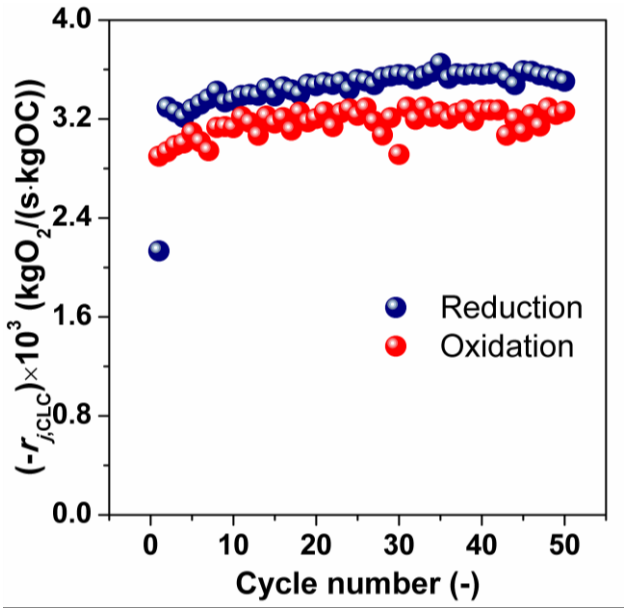

Fig. 5. Reaction rates of reduction and oxidation change as a function of cycle numbers during the redox by 15 vol.% H_2 and 100 vol. % air at 950 ^oC.

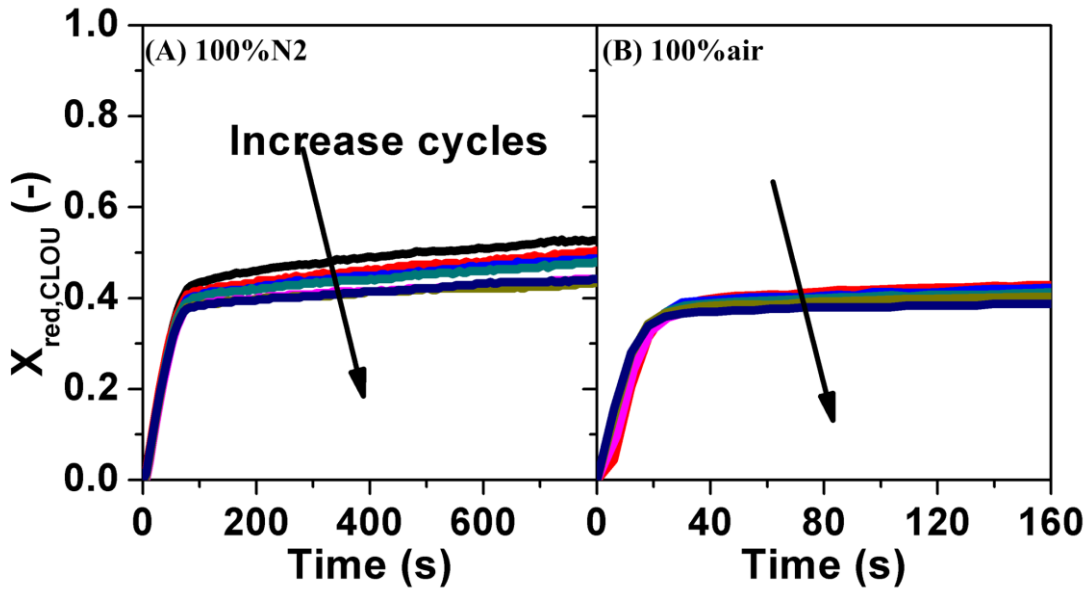

Fig. 6. Oxygen carrier conversions as a function of time during 10 cycles with (A) 100 vol.% N_2 and (B) 100 vol.% air; tests were conducted at 950 ^{o}C; Calculated using R_{OC} = 5.5 wt.%.

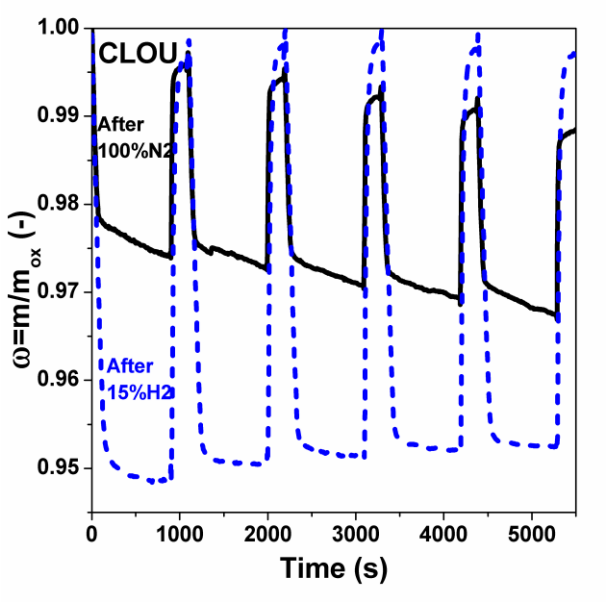

Fig. 7. Mass variations in CLOU process in cycles alternating N_2 and air for fresh $CuO/CuAl_2O_4$ (black line) and for particles after redox cycles with 15 vol.% H_2 (blue line). The operation temperature is 950 ^oC.

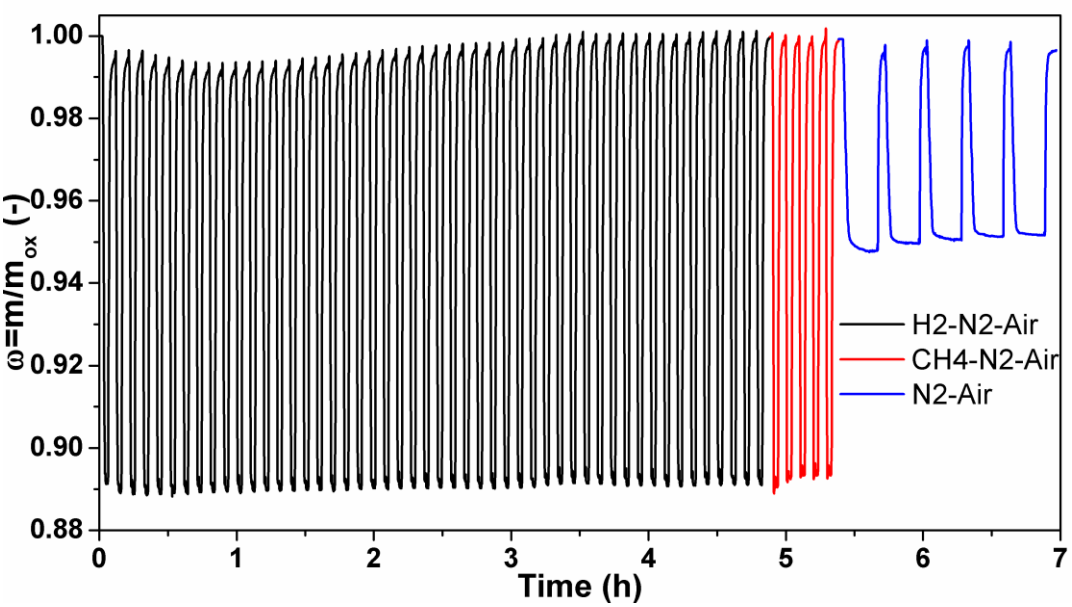

Fig. 8. Mass variations as a function of the reaction time for $CuO/CuAl_2O_4$ during 50 redox cycles with 15 vol.% H_2, followed by 5 cycles with 15 vol.% CH_4+20%H_2O and then 5 cycles with 100 vol.% N_2 at 950 ^oC; oxidation periods were conducted with 100 vol.% air.

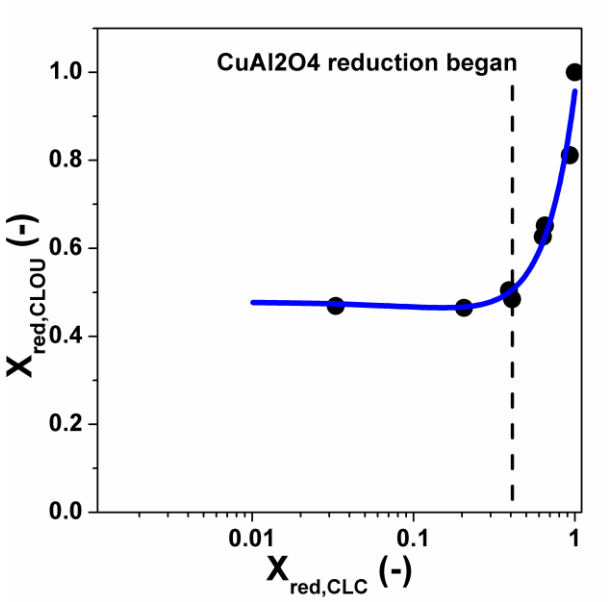

Fig. 9. Solid conversions in 100 vol.% N_2, $X_{red,CLOU}$, as a function of the reduction degree $X_{red,CLC}$ with gaseous fuels attained in previous redox cycles; Temperature: 950 ^{o}C; $R_{OC,CLOU}$ = 5.5 wt.%.

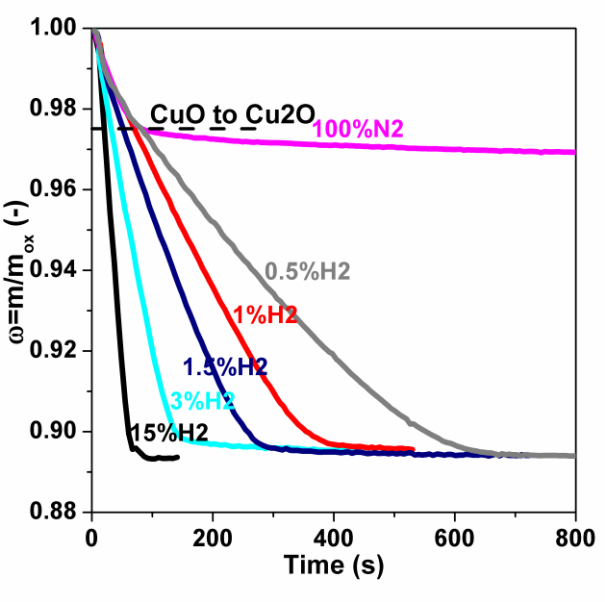

Fig. 10. Effects of H_2 concentration on the reduction of the $CuO/CuAl_2O_4$ oxygen carrier; Temperature: 950 ^oC.

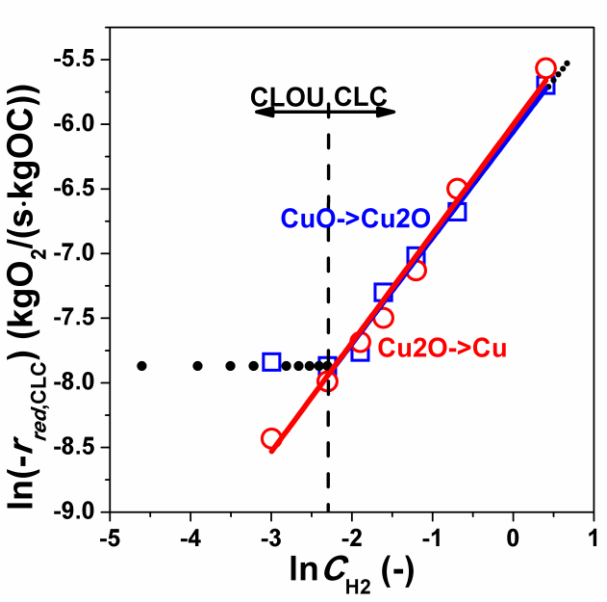

Fig. 11. Reduction rates of $CuO/CuAl_2O_4$ as a function of the H_2 concentration.

Table Captions

Table 1. Composition of the $CuO/CuAl_2O_4$ oxygen carrier prepared by sol-gel method.

Table 1. Composition of the $CuO/CuAl_2O_4$ oxygen carrier prepared by sol-gel method.

Elements (wt.%)	**by ICP-AES**	**by TGA tests**
Cu	44.8	43.7
Al	21.7	24.0[a]
O	33.5	32.3
Compounds (wt.%)[b]		
CuO		21.9
$CuAl_2O_4$		78.1
XRD main phases		
Fresh	CuO, $CuAl_2O_4$	
Used in N_2	Cu_2O, $CuAlO_2$, $CuAl_2O_4$	
Used in H_2 or CH_4	Cu, θ-Al_2O_3	

[a] by difference; [b] for fresh particles